GANIL

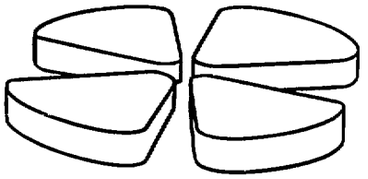

THE PRINCIPLE OF THE HBT EFFECT AND ITS APPLICATIONS IN NUCLEAR PHYSICS

Y. SCHUTZ

GANIL, BP 5027 14021 CAEN-CEDEX France

Cours donné au TAPS Workshop, Schiermonikoog (NL), 10-14 septembre 1990

GANIL P 90 22

THE PRINCIPLE OF THE HBT EFFECT AND ITS APPLICATIONS IN NUCLEAR PHYSICS

Y. SCHUTZ

GANIL, BP 5027 14021 CAEN-CEDEX France

Cours donné au TAPS Workshop, Schiermonikoog (NL), 10-14 septembre 1990

THE PRINCIPLE OF THE HBT EFFECT AND ITS APPLICATIONS IN NUCLEAR PHYSICS .

Y. SCHUTZ
GANIL BP 5027
14021 Caen-Cedex, France

November 7, 1990

Abstract

The principle of intensity interferometry, as it was first stated by Hanbury-Brown and Twiss, will be developed. The discussion will be illustrated by its application in astronomy. Strong emphasis will be put on the particularities of intensity interferences when compared to classical interferences. It will be shown how in nuclear Physics the effects observed in the correlation of identical particles can be interpreted in terms of intensity interferences. A broad review of the existing data is presented.

In 1954, R. Hanbury-Brown and R.Q. Twiss stated [3] the principle of a new kind of radio-interferometer designed to improve the resolution of existing interferometers. Later, they showed [4] that the principle is a universal one and that the effects can be observed with light sources. A few years later [8] the interpretation of enhancement observed in the correlations of like-sign pions relative to unlike-sign pions invoked the same principle. This discovery has triggered a lot of experiments in nuclear physics. It is now a commonly used technique to measure the spatial and temporal extension of the sources of the particles created in particle and nuclear collisions.

In the first part of this lecture I will describe the principle of second order interference and compare it with classical interferences. The development will be illustrated with its application to astronomy.

The second part will explain what is understood by HBT effect in nuclear physics and show how space-time information of particle or nuclear collisions can be extracted from particle correlations. This section will be illustrated by data obtained to date.

1 Conventional interference and the HBT effect

Fundamentally any experiment which superimposes electromagnetic fields can be called an interference experiment. In classical optics, interference has received a more restrictive definition as the observation of a stationary intensity pattern (the fringes) produced by two conveniently prepared light waves. The quantum mechanical interpretation of what I shall call conventional interference experiments has been given by Dirac[1] as "*the interference of the photon with itself*". Dirac continues by stating that "*interference between two different photons never occurs*". Whereas the first statement is true, the second is not correct. In fact, as we shall see, the HBT effect results from the superposition of two independent photons, and differs fundamentally from classical interferences known by Dirac. Nevertheless, it can still be considered as an interference effect, and is often referred to as second order interference.

To have a better understanding of the pecularities of the second order interference effects, I will first recall the basics of classical interference.

1.1 The "YOUNG" experiment

Monochromatic light from a part source S illuminates a dark screen S_1 with two tiny identical holes h_1 and h_2 separated by a distance L. At a distance D and perpendicular to S_1 is a black screen S_2 on which we observe the effect (see figure 1.).

Let us describe the light by its electric field which we write as a plane wave linearly polarized:

$$E = E_0 \exp i\left(\vec{k}\cdot\vec{r} - \omega t - \phi\right) \tag{1}$$

where E_0 is the amplitude, $\vec{k}$ the wave vector, ω the circular frequency and ϕ the phase. At the point P on the screen S_2 we classically overlay the amplitudes originating from h_1 and h_2:

$$\begin{aligned} h_1 &: E_1 = E_0 e^{i(\vec{k}\vec{r_1} - \omega t - \phi_1)} \\ h_2 &: E_2 = E_0 e^{i(\vec{k}[\vec{r_1}+\vec{\delta}] - \omega t - \phi_2)} \end{aligned}$$

The experiment is set up so that the light travels along the same distance from the source S to both holes. If the screen S_2 is at a distance much larger than the distance between the two holes ($D >> L$) the path difference δ between E_1 and E_2 can be approximated to:

$$\delta \simeq \frac{Lx}{D}$$

where x is the coordinate of P on the screen S_2. On S_2 we observe the intensity of the superposition field which from the classical definition is the square of its amplitude :

$$\begin{aligned} I_p(x) &= |E_1 + E_2|^2 \\ &= E_0^2 \cdot \left(2 + e^{i\vec{k}\cdot\vec{\delta}}\right) \\ &= 2E_0^2 \cdot \left(1 + \cos\left[\vec{k}\cdot\vec{\delta}\right]\right) \\ &= 2E_0^2 \cdot \left(1 + \cos\left[\frac{2\pi}{\lambda}\frac{L}{D}x\right]\right) \end{aligned} \tag{2}$$

λ being the wavelength.

The intensity varies periodically along the screen S_2 and shows a succession of maxima and minima, the fringes, with a periodicity of $\frac{\lambda D}{L}$.

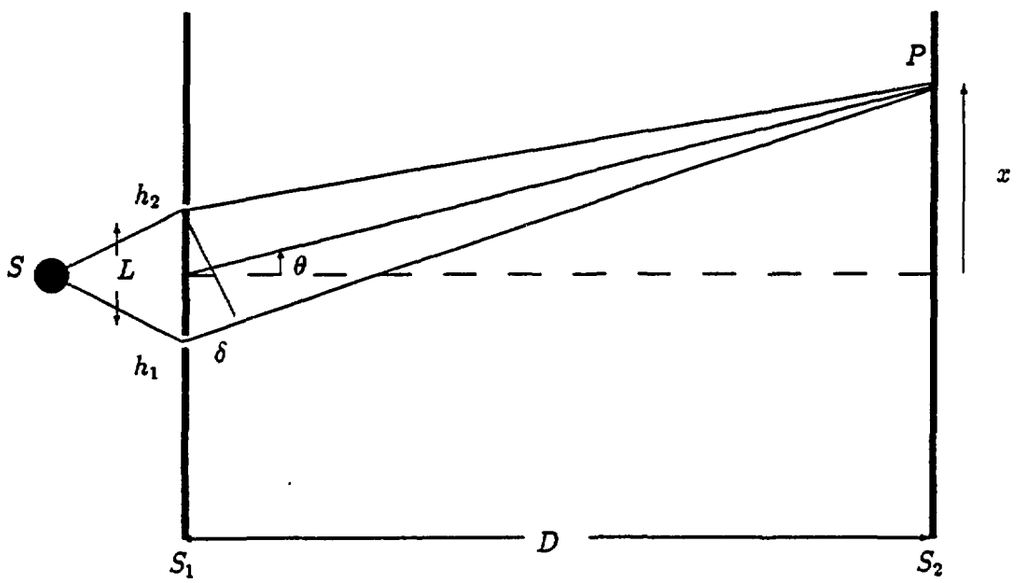

Figure 1. *Schematic set-up of the Young experiment.*

In Quantum Mechanics, the electrical field is described by an hermitian operator $\vec{E}(\vec{r}, t)$. If we denote by $a_i^\dagger$ the creation operator for the mode of a photon coming out of hole $h_i (i = 1, 2)$ and a_i the corresponding annihilation operator, the quantum states $|n>$ of the n-photon mode, can be written as :

$$|n> = (n!)^{-\frac{1}{2}} \cdot \left(a^\dagger\right)|0>$$

We have assumed that the two holes are identical, so that the resulting mode has the operators:

$$\begin{aligned} a^\dagger &= (a_1^\dagger + a_2^\dagger)/\sqrt{2} \\ a &= (a^\dagger)^\dagger \end{aligned}$$

The superposition field at P on the screen S_2 is then written as the operator E_p:

$$E_p(\vec{r},t) = a_1 e^{i(\vec{k}\vec{r_1}-\omega t-\phi_1)} + a_2 e^{i(\vec{k}[\vec{r_1}+\vec{\delta}]-\omega t-\phi_1)}$$

The observed intensity can be written as the mean value of an intensity operator $I_p(\vec{r})$, the photon-number operator of the mode which we define as follows:

$$\begin{aligned} < n|I_p(\vec{r})|n > &= < n|E_p^\dagger(\vec{r},t)\cdot E_p(\vec{r},t)|n > \\ &= < n|a_1^\dagger \cdot a_1|n > + < n|a_2^\dagger \cdot a_2|n > + 2\cos\left(\vec{k}\cdot\vec{\delta}\right)\cdot < n|a_1^\dagger \cdot a_2|n > \end{aligned}$$

where we have made use of the following commutation relation:

$$[a_1^\dagger, a_2] = [a_2^\dagger, a_1]$$

Since $a_i^\dagger \cdot a_i$ is the operator which counts the number of photons emerging from hole h_i, we can rewrite the intensity as:

$$< n|I_p(\vec{r})|n >= n\left(1+\cos\vec{k}\cdot\vec{\delta}\right)$$

It follows from the expressions for the intensity distribution on the screen that it is equivalent to do the experiment with n incident photons or to repeat n times the experiment with a single photon. This is equivalent to Dirac's statement "*each photon interferes (only) with itself*". Indeed, it has been checked experimentally [2] that a visible interference pattern can still be observed when the light intensity is so low that the delay between successive photons is much longer than the transit time through the apparatus.

Let us now generalize the Young experiment by considering the superposition of two monochromatic traveling plane waves linearly polarized in the same direction. As before we consider only the electric field at coordinate $(\vec{r},t)$:

$$E_j(\vec{r},t) = E_j e^{i(\vec{k_j}\vec{r}-\omega_j t-\phi_j(t))} \quad j=1,2$$

The field is not strictly monochromatic since only E_j is constant and the phases ϕ_j fluctuate in time. As before we derive the intensity in the superposition field :

$$I(\vec{r},t) = E_1^2 + E_2^2 + 2E_1E_2\cos\left[\left(\vec{k_2}-\vec{k_1}\right)\cdot\vec{r} - (\vec{\omega_2}-\vec{\omega_1})\cdot t - (\phi_2(t)-\phi_1(t))\right] \qquad (3)$$

In order to observe a standing spatial interference pattern it is necessary to have $\omega_1 = \omega_2$ and the phase difference $\phi_2(t)-\phi_1(t)$ needs to remain constant during a time interval which is of the order of the length of the observation time. This leads to the definition of coherent light, light whose phase and amplitude remain constant in a time interval long enough for an actual observation to be made, and the coherence length, the length in the direction of the beam propagation over which the phase and amplitude remain constant. Thus strictly speaking, we deduce from relation 3 that it is not necessary to have two coherent fields to produce an interference pattern, but it is sufficient that the fluctuations of ϕ_1 and ϕ_2 are not independent and that the path difference remains constant over the coherence length. These conditions are obtained in the Young experiment by splitting the light into two identical components.

1.2 The Michelson interferometer

Conventional interference effects were used in astronomy to measure the angular size of visible or radio-emitter stars. The device is one of several "Michelson" interferometers and I will describe in details how it works. This will be very useful in order to show the differences with an intensity interferometer. Figure 2 shows a simplified diagram of a Michelson radio interferometer. Two aerials A and B separated by a distance L are oriented in the direction of the radio-source. The signals detected by A and by B are added through a cable, and fed to a receiver at equal distance from A and B whose intensity output is recorded.

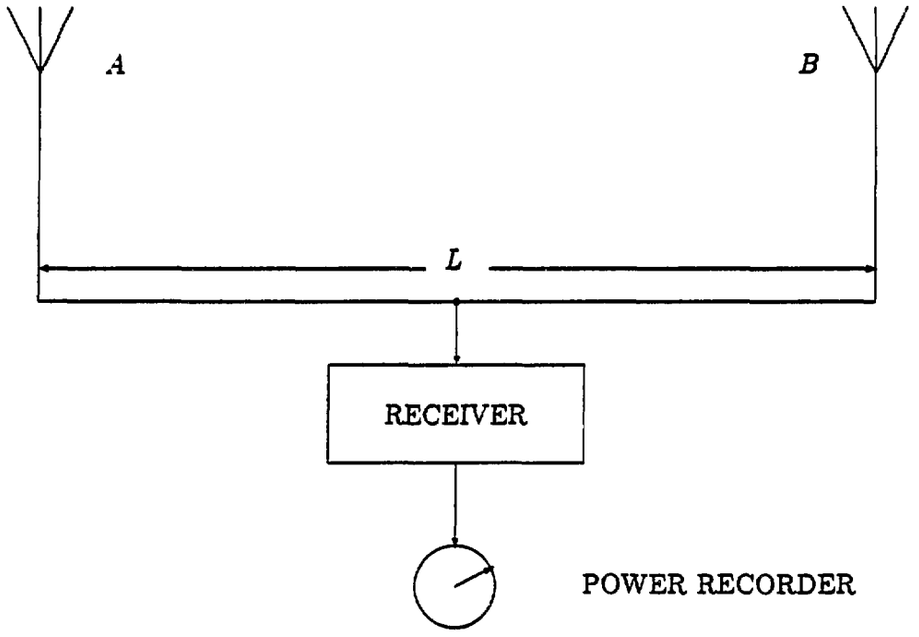

Figure 2. *Simplified diagram of a Michelson type radio-interferometer.*

Let us consider the simple case of an imaginary star represented in figure 3 by a narrow strip coplanar with the baseline AB of the interferometer. As in the Young experiment, we can easily deduce the relative phase δ between A and B from a radiating element P on the star assuming that the distance to the star is much larger than the distance between the two aerials:

$$\delta = \frac{\omega_0}{c} L \sin(\theta_0 + \theta)$$

ω_0 is the angular frequency to which the receiver is tuned and the angles θ_0 and θ are defined on figure 3. From relation 2 we deduce that from P we measure at the output of the receiver a quantity I_p which is proportional to :

$$I_p \propto I_p(\theta) d\theta \cos\left[\frac{\omega_0 L}{c} \sin(\theta_0 + \theta)\right]$$

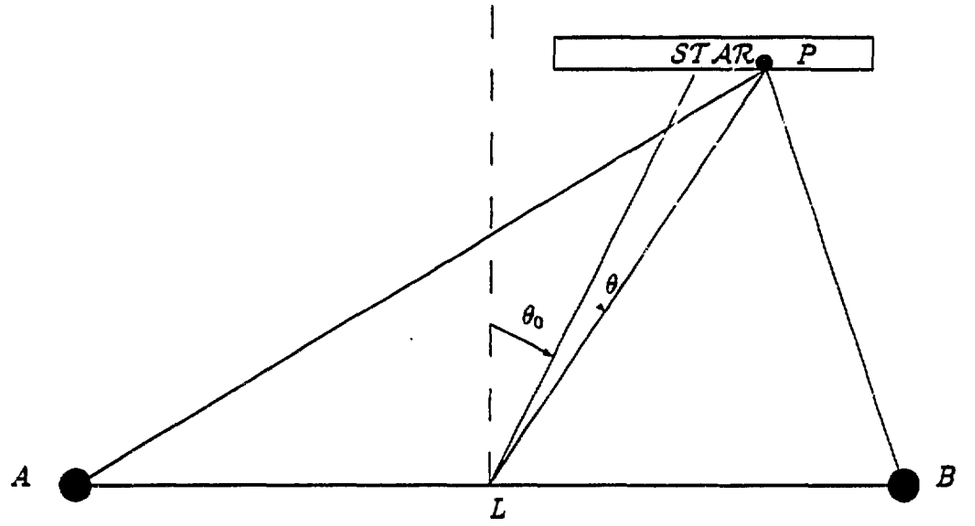

Figure 3. *Principle of the Michelson type interferometer.*

where $I_p(\theta)d\theta$ is the intensity received from the element P. The receiver output due to the whole source is proportional to:

$$I \propto \int_{-\frac{\alpha}{2}}^{\frac{\alpha}{2}} I_p = \int_{-\frac{\alpha}{2}}^{\frac{\alpha}{2}} I_p(\theta)d\theta \cos\left[\frac{\omega_0 L}{c}\sin(\theta_0+\theta)\right]$$

where α is the maximum extension of the star. Since α is generally small enough so that one can use the approximations : $\sin\theta \sim \theta$, $\cos\theta \sim 1$. The intensity I can be written as proportional to:

$$I \propto \mathcal{F}_1 \cdot \cos\left(\frac{\omega_0 l}{c}\tan\theta_0\right) - \mathcal{F}_2 \cdot \sin\left(\frac{\omega_0 l}{c}\tan\theta_0\right)$$

where we have defined $\mathcal{F}_1$, $\mathcal{F}_2$ and l as :

$$\begin{aligned}
\mathcal{F}_1 &= \int_{-\frac{\alpha}{2}}^{\frac{\alpha}{2}} I(\theta)\cos\left(\frac{\omega_0 l}{c}\theta\right)d\theta \\
\mathcal{F}_2 &= \int_{-\frac{\alpha}{2}}^{\frac{\alpha}{2}} I(\theta)\sin\left(\frac{\omega_0 l}{c}\theta\right)d\theta \\
l &= L\cos\theta_0
\end{aligned}$$

Since the star moves relative to the interferometer, θ_0 varies with time and the output of the receiver oscillates sinusoidally as the angle θ_0 (or the time) varies. The amplitude and the phase of the oscillations are related to the Fourier transform ($\mathcal{F}_1$,$\mathcal{F}_2$) of the angular distribution of the intensity across the star. Thus it should be possible to determine, from the relative amplitudes and phases obtained in identical measurements by changing the length of the baseline L, the shape of the star (at a given frequency). It is only true in principle since measuring a relative phase is experimentally difficult and one ends up by making assumptions about the general shape of the star.

The resolving power of the Michelson interferometer is of the order of λ/L. It can be optimized either by selecting short wavelength or by extending the baseline length L. The baseline is limited to a few hundred meters by attenuation in the cable. It is not always practicable to select too short wavelength because the intensity of the stars diminishes with decreasing λ. On the other hand it is desirable to measure the effective diameter of the star as a function of λ. Because of these limitations Hanbury-Brown and Twiss developed a new kind of interferometer, the intensity interferometer which I will describe next.

1.3 The intensity interferometer

Figure 4 depicts a simplified diagram of the intensity interferometer as proposed by Hanbury-Brown and Twiss [3].

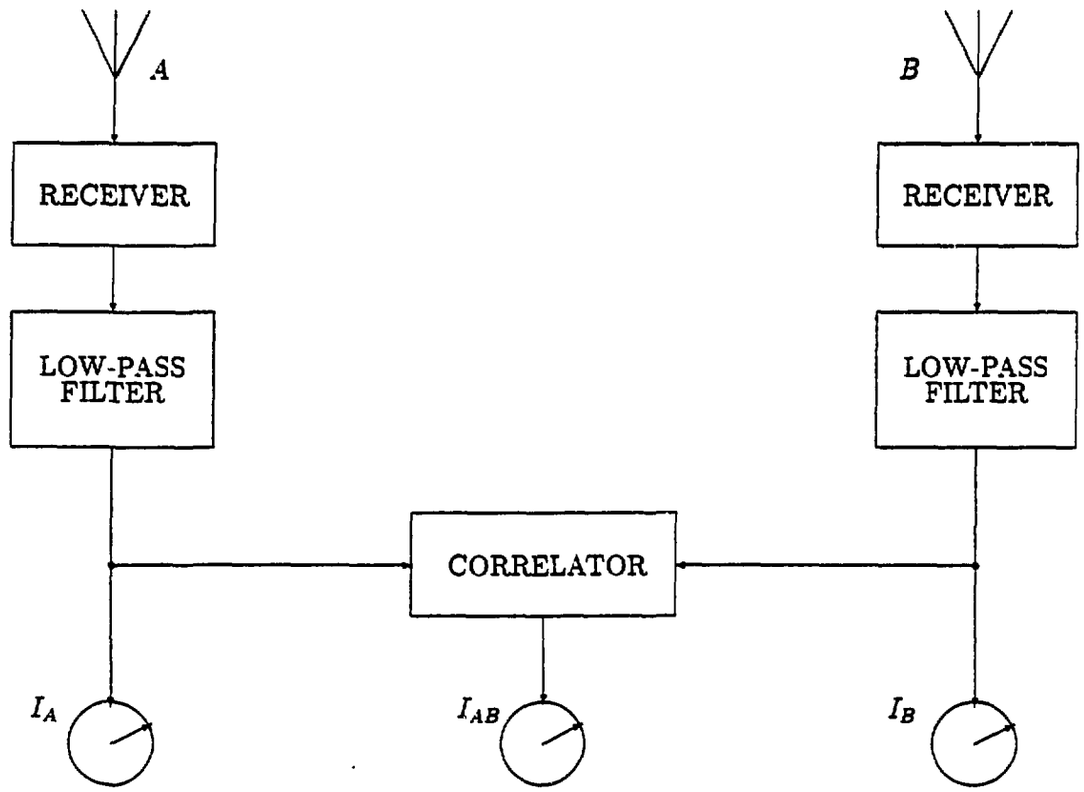

Figure 4. *Simplified diagram of a Intensity radio-interferometer.*

In contrast to the Michelson interferometer the signal from the two aerials A and B are fed into two independent receivers having identical band-width characteristics and tuned to the same frequency. The power output of each receiver is passed through low-pass filters before feeding a correlator whose output I_{AB} is recorded. At the same time, the output of the low-pass filters I_A and I_B are recorded independently. A typical record measured during the transit of a star is displayed on figure 5. The intensities I_A and I_B show an identical variation with time and can be decomposed into an uniform background (due to cosmic noise and to the noise of the receiver and the signal power received from the

star. The output of the correlator (I_{AB}) shows only the signal from the star since the two receivers are independent and the cosmic noise measured in the two aerials is uncorrelated.

We shall now see how, as for the Michelson interferometer, I_{AB} can be related to the intensity distribution in the star. We will consider an hypothetical star made of a narrow strip coplanar with the baseline AB (fig. 6). In the Michelson interferometer we have considered the radiation at a single frequency emerging from a single point in the star. Two signals coming from two different points or signals with different frequencies could be neglected since they are uncorrelated. For the intensity interferometer, we have to consider signals at different frequencies ω_i emerging from different points P_i in the star. To simplify we will consider only two points P_1 and P_2 in the star at angles θ_1 and θ_2.

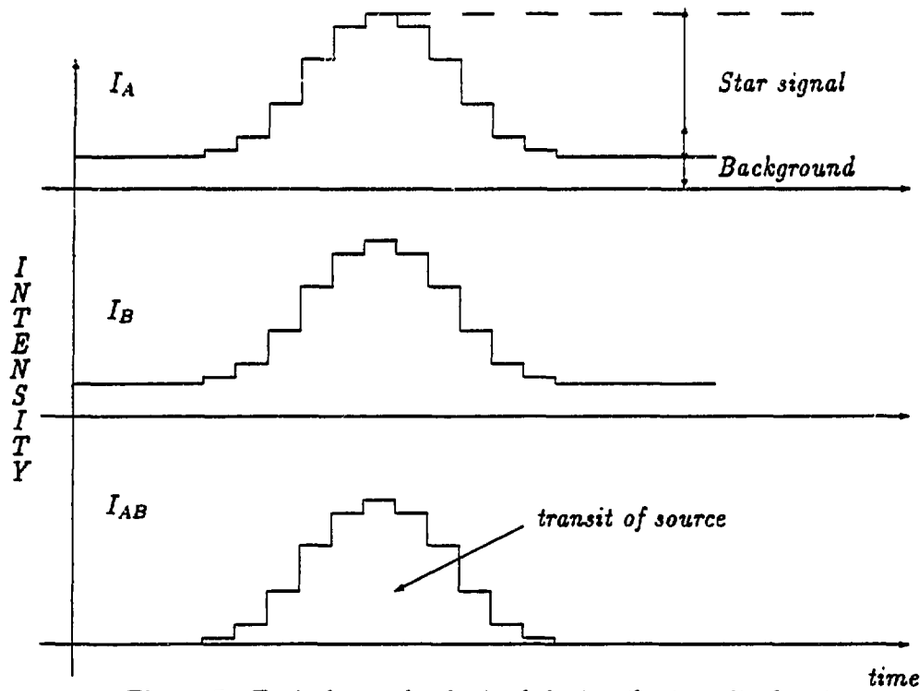

Figure 5. *Typical records obtained during the transit of a star from an intensity interferometer.*

We will limit the discussion to the electric field radiated from P_i and represent it by a plane-wave linearly polarized:

$$E_i = E_i^0 e^{i(\vec{k}_i \vec{r}_i - \omega_i t - \phi_i)} \quad i = 1, 2$$

The intensity seen by A is due to the interaction of the field originating from P_1 and P_2:

$$\begin{aligned} I_A &= |E_{1A} + E_{1B}|^2 \\ &= \left\{ E_1^0 e^{i(\vec{k}_1 \vec{r}_1 - \omega_1 t - \phi_1)} + E_2^0 e^{i(\vec{k}_2 \vec{r}_2 - \omega_2 t - \phi_2)} \right\}^2 \end{aligned}$$

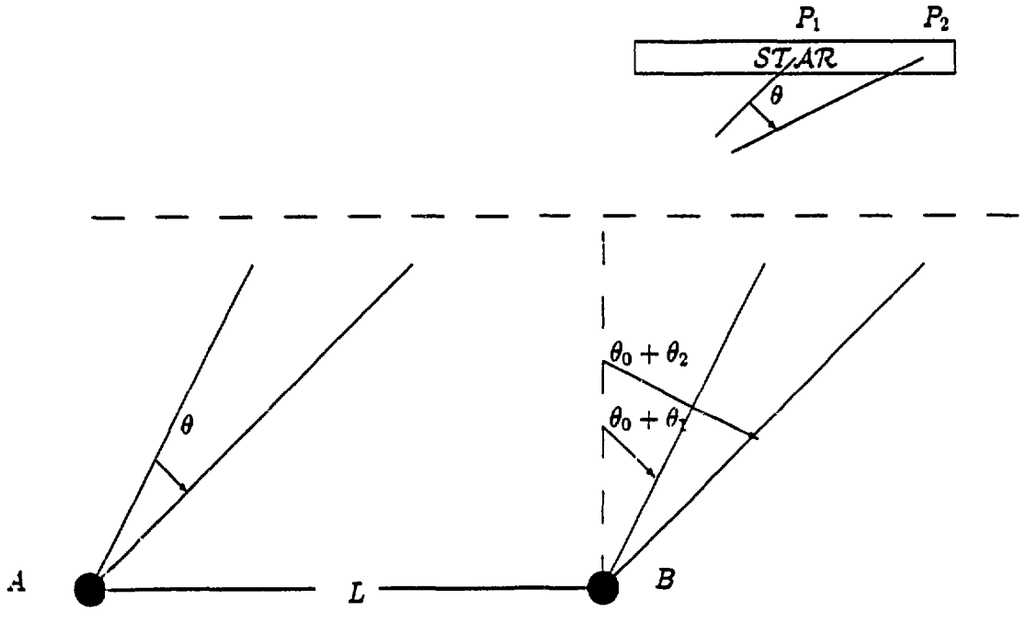

Figure 6. *Principle of the intensity interferometer.*

The low-pass filter eliminates the high-frequency components so that the output from A becomes:

$$\begin{aligned} I_A &= E_1^{0^2} + E_2^{0^2} + 2E_1^0 E_2^0 \cos\left[\vec{k_1}\vec{r}_{1A} - \vec{k_2}\vec{r}_{2A} - (\omega_1 - \omega_2)\,t - (\phi_1 - \phi_2)\right] \\ &= E_1^{0^2} + E_2^{0^2} + 2E_1^0 E_2^0 \cos\left[-(\omega_1 - \omega_2)\,t + \delta_A - (\phi_1 - \phi_2)\right] \end{aligned} \tag{4}$$

The path difference δ_A between the radiation traveling from P_1 to A and P_2 to A is :

$$\begin{aligned} \delta_A &= \vec{k}_{1A}\vec{r}_{1A} - \vec{k}_{2A}\vec{r}_{2A} \\ &= \frac{R_0}{c}\left\{(\omega_1 - \omega_2)\cdot\left(1 + \frac{L\sin\theta_0}{2R_0}\right) + \frac{L\cos\theta_0}{2R_0}\cdot(\theta_1\omega_1 - \theta_2\omega_2)\right\} \end{aligned}$$

Where we have made use of the following approximations $\tan\theta_2 \sim \sin\theta_{1,2} \sim \theta_{1,2}$. The definition of the parameters is found in fig. 6.

Similar expressions can be written for the intensity seen at the output of receiver B

$$I_B = E_1^{0^2} + E_2^{0^2} + 2E_1^0 E_2^0 \cos\left[-(\omega_1 - \omega_2)t) + \delta_B - (\phi_1 - \phi_2)\right]$$

and

$$\delta_B = \frac{R_0}{c}\left\{(\omega_1 - \omega_2)\cdot\left(1 + \frac{L\sin\theta_0}{2R_0}\right) + \frac{L\cos\theta_0}{2R_0}\cdot(\theta_1\omega_1 - \theta_2\omega_2)\right\}$$

The phase difference between the signal seen by A and the signal seen by B is:

$$\begin{aligned} \delta &= \delta_A - \delta_B \\ &= \frac{(\omega_1 - \omega_2)\,L\sin\theta_0}{2c} + \frac{L\cos\theta_0}{2c}(\theta_1\omega_1 - \theta_2\omega_2) \end{aligned}$$

The first term in the preceding sum is the difference in the time of arrival of the signals at A and B and can be made experimentally equal to zero. When the frequency $(\omega_1 - \omega_2)$ lies within the band width of the low-pass filter the following signals are fed to the correlator:

$$\begin{aligned} I_A &\propto \cos\{(\omega_2 - \omega_1)\,t - (\phi_1 - \phi_2)\} \\ I_B &\propto \cos\{(\omega_2 - \omega_1)\,t - (\phi_1 - \phi_2) + \delta\} \end{aligned}$$

The time integrated output of the correlator is:

$$I_{AB} = \overline{I_A \cdot I_B} = \frac{1}{T}\int_t^{t+T} I_A \cdot I_B \, dt$$

where T is the integration time. The integral can be easily evaluated and by requiring that $T >> \frac{2\pi}{\omega_2 - \omega_1}$ and $\omega_1 \simeq \omega_2 = \omega$ (low-pass filter):

$$I_{AB} \propto \cos\left\{\frac{2\pi}{\lambda} L\,(\theta_1 - \theta_2)\right\} \tag{5}$$

We can thus see that, although all informations about the absolute phase in either aerial is lost, information about the angular size $(\theta_1 - \theta_2)$ of the star is preserved by the relative phase in the detector outputs and therefore is contained in the output of the correlator. That leads us also to the following very important remark: the source has to be incoherent i.e. the points on the star must radiate independently of each other or with randomly fluctuating relative phase.

We could generalize the preceding derivation of I_{AB} to the whole source. As in the case of Michelson interferometer we would find that the intensity I_{AB} is proportional to the Fourier transform of the intensity distribution across the source. The shape and the size of the source is then deduced from several measurements with various baseline lengths. What makes such a kind of interferometer more attractive than the Michelson interferometer is its great potential resolving power, since the baseline length can be made much longer, and also the fact that the atmospheric noise is eliminated. Nevertheless, this method can only be applied to the most brilliant stars.

Hanbury-Brown and Twiss have shown [4] that the same method can be applied to visible stars when the two aerials are replaced by photomultipliers [5]. The correlator in that case counts the number of coincidences between the two photomultipliers. A normalized correlation function is defined as the ratio of the number of coincidences to the single rates in each photomultipliers:

$$C(L) = \frac{I_{AB}}{I_A \cdot I_B}$$

From relation 5 we see that the width of this correlation function can be shown to be inversely proportional to the angular diameter of the star. The normalized correlations function measured [6] with the stellar interferometer at Narrabri Observatory for three stars of different angular size are shown on fig. 7. The solid lines on the figure were fitted to the experimental points by assuming the shape of the star to be an uniformly illuminated disk. The deduced angular diameters are reported on the figure.

1.4 Intensity interference

The so called HBT effect differs fundamentally from conventional interference where the occurrence of a stationary intensity pattern is due to the superposition of the amplitudes

of two coherent light waves having the same frequency:

$$I_{A+B} = |E_A + E_B|^2$$

It is necessary to have the same frequency in order to observe a stationary pattern. The coherence condition means that although the phase of each wave can fluctuate, the relative phase must remain constant. On the contrary, the HBT effect is observed in the correlation of two independent light waves having different frequencies and having phases which fluctuate randomly with respect to each other:

$$I_{A\cdot B} = I_A \cdot I_B = E_A^2 \cdot E_B^2$$

According to the basic definition of interference, as a superposition of electromagnetic fields, the intensity correlation observed by Hanbury-Brown and Twiss can be called an interference effect, but of a very new type since the interference occurs between photons spontaneously emitted by different atoms (on the surface of the star). Therefore the HBT effect is also commonly called second order interference, intensity interference (as opposed to amplitude interference) or as intensity correlation. It is a two-photon effect and accordingly is an effect Dirac didn't dream of in 1930.

It is usual to define a correlation function [7] C as the average over an ensemble of the product of the intensities of the two waves

$$C(\vec{r_1}, \vec{r_2}) = \overline{I_A \cdot I_B}$$

From relation 4 and by assuming that the two waves have equal intensities, $E_1^{0^2} = E_2^{0^2} = I$, the correlation function becomes:

$$C(\vec{r_1}, \vec{r_2}) = \bar{I}^2 \left\{ 1 + \frac{1}{2} \cos \left[\left(\vec{k_1} - \vec{k_2} \right) \cdot \left(\vec{r_1} - \vec{r_2} \right) \right] \right\}$$

where $\bar{I} = E_1^{0^1} + E_1^{0^2} = 2I$ is the mean intensity. The correlation function is a maximum when the path difference $|\vec{r_2} - \vec{r_1}| = 0$ and decreases with increasing path difference until a constant level is reached. This behaviour can be compared with the decrease of fringe visibility in the Young experiment when the distance between the two holes increases .

If now we consider photons instead of waves, one may wonder why two independently emitted photons have an enhanced probability to arrive at a short relative separation. This correlation cannot be understood if one regards a photon as a classical particle which one can follow from its creation up to its detection. In fact, what is registered as a photon in the photomultiplier is an energy packet $h\nu$ taken from the superposition field of the emitted photons. It is therefore clear why the individual photon carries information on both fields. Therefore, we may state that the HBT affect results from the interference of two independent photons.

These considerations lead us to the next chapter where I will describe how, in nuclear physics, correlations between identical particles can be interpreted similarly to the HBT effect and how source sizes can be extracted. I will then extend the discussion to other effects, peculiar to nuclear physics, which also give rise to strong correlation effects but have nothing to do with intensity interference.

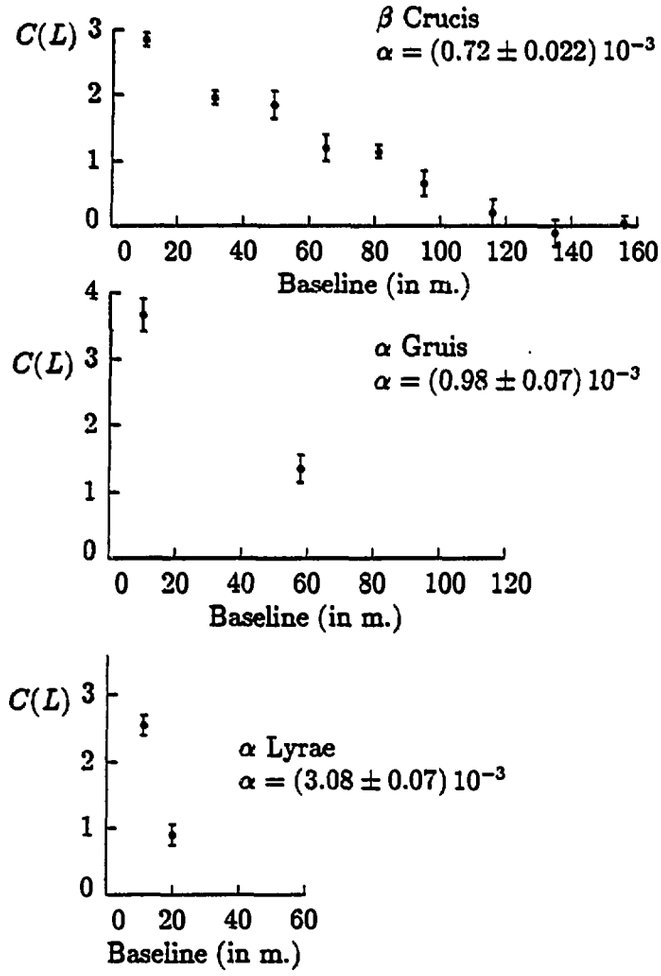

Figure 7. *Correlation function versus baseline length for three stars of different angular size. From ref. [6].*

2 Two-particle correlations in nuclear physics

The first evidence for particles emitted with enhanced probability at small relative momenta was found by chance by S. Goldhaber et al. [8] as they studied the ρ meson through its $\pi^+\pi^-$ decay in $p\bar{p}$ collisions. They discovered that pairs of equally charged pions show a higher probability for emission with small opening angles than pairs of oppositely charged pions. The effect has been interpreted in terms of the extension of the pion source and given the name of GGLP effect [9].

The interpretation of the effect is thus very similar to the HBT effect. But there is an essential difference: whereas in astrophysics the emission can be assumed to be stationary during the observation time, in nuclear physics the system is evolving with time. Therefore, both the spatial and temporal extension of the source can be investigated through the study of the correlation of identical particles.

2.1 HBT effect in identical particle correlations

In high energy particle physics, where pions are the most abundant reaction products, particle correlations have been studied almost exclusively between charged pions. Therefore, one often identifies the HBT effect with Bose-Einstein correlation. But similar effects also exist if one considers instead of bosons, fermions such as protons which are more abundant at low and intermediate heavy-ion energies. It is essential that the two particles are identical since, as I will now show , the effect results from the symmetry of the wave function for a system of identical particles.

Let us consider particles emitted from a source having the density distribution $\rho(\tilde{r})$. The density distribution does not vary with time, since the particles will give a picture of the freeze-out density of the source, i.e. the stage of expansion when the interaction between particles ceases. The particles are detected at d_1 and d_2 (see fig. 8).

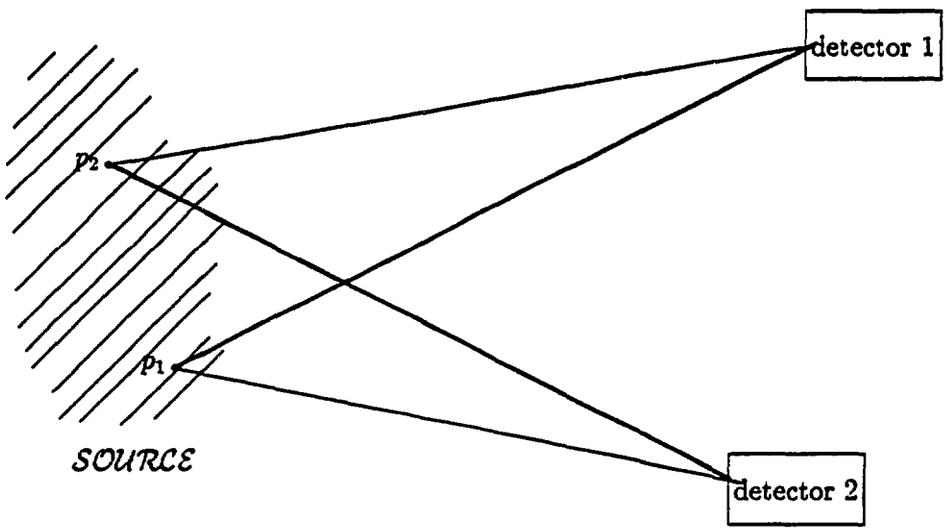

Figure 8. *Detection of two identical particles.*

We now evaluate the correlation coefficient defined as :

$$C_{12}(\tilde{q}) = \frac{P(\tilde{p}_1, \tilde{p}_2)}{P(\tilde{p}_1)\,P(\tilde{p}_2)} - 1 \tag{6}$$

where $\tilde{q}$ is the relative four-momentum of the two particles, $P(\tilde{p}_1, \tilde{p}_2)$ is the two-particle probability density and $P(\tilde{p}_i)$ is the single particle probability density with four-momentum $\tilde{p}_i$. If we assume that the particles are emitted from a chaotic source, the two-particle probability density can be written as an incoherent sum over the source of the amplitudes $(\Psi_{12}(\tilde{p}_1, \tilde{p}_2))$ for a particle pair produced at p_1 and p_2 and registered in detectors d_1 and d_2 (see fig.8):

$$P(\tilde{p}_1, \tilde{p}_2) = \int_{\text{source}} |\Psi_{12}(\tilde{p}_1, \tilde{p}_2)|^2\, \rho(\tilde{r_1})\, \rho(\tilde{r_2})\, d^4r_1 d^4r_2 \tag{7}$$

Since the two particles are indistinguishable we are unable to determine whether the particle detected in d_1 was emitted from p_1 or p_2. One needs therefore to add the two contributions

represented by the thick and thin lines in fig. 8.

$$\Psi_{12}(\tilde{p}_1, \tilde{p}_2) = \frac{1}{\sqrt{2}} \{\Psi(\tilde{p}_1, \tilde{p}_2) \pm \Psi(\tilde{p}_2, \tilde{p}_1)\} \tag{8}$$

The plus-sign in equation 8 is for a system of bosons for which the wave function is symmetric with respect to exchange of particles and the minus sign for a system of fermions. $\Psi(\tilde{p}_1, \tilde{p}_2)$ ($\Psi(\tilde{p}_2, \tilde{p}_1)$) is the probability amplitude for detection in d_1 of the particle emitted from $p_1(p_2)$ with four-momentum $\tilde{p}_1(\tilde{p}_2)$ and in d_2 of the particle emitted from $p_2(p_1)$ with four-momentum $\tilde{p}_2(\tilde{p}_1)$. We have assumed that the particles travel as free particles after their emission and we describe the wave-functions by plane-waves :

$$\begin{aligned} \Psi(\tilde{p}_1, \tilde{p}_2) &= e^{i\tilde{p}_1\tilde{r}_1} \cdot e^{i\tilde{p}_2\tilde{r}_2} \\ \Psi(\tilde{p}_2, \tilde{p}_1) &= e^{i\tilde{p}_2\tilde{r}_1} \cdot e^{i\tilde{p}_1\tilde{r}_2} \end{aligned} \tag{9}$$

where $\tilde{r}_i$ is the four-vector $(\vec{r}_i, t)$. Using the definitions 8, and 9, we can rewrite 7 as:

$$\begin{aligned} P(\tilde{p}_1, \tilde{p}_2) &= \int_{\text{source}} R(\tilde{r}) \cdot R^*(\tilde{r})\, d^4\tilde{r} d^4\tilde{r} \\ &\pm \int_{\text{source}} R(\tilde{r})\, e^{i(\tilde{p}_1 - \tilde{p}_2)\tilde{r}} d^4\tilde{r} \cdot R^*(\tilde{r})\, e^{-i(\tilde{p}_1 - \tilde{p}_2)\tilde{r}} d^4\tilde{r} \\ &= |\mathcal{F}[R(0)]|^2 \pm |\mathcal{F}[R(\tilde{q})]|^2 \end{aligned}$$

with the following definitions, $R(\tilde{r}) = \rho(\tilde{r_1}) \cdot \rho(\tilde{r_2})$, $\tilde{q} = (\tilde{p}_1 - \tilde{p}_2)$ is the relative four-momentum and $\mathcal{F}[R(\tilde{q})] = \int_{\text{source}} R(\tilde{r})\, e^{(i\tilde{q}\tilde{r})} d^4\tilde{r}$ is the Fourier transform of the source density distribution. The denominator in the definition 6 of the correlation coefficient can be written in the same way:

$$P(\tilde{p}_i) = \int_{\text{source}} \rho(r_i) \left| e^{(i\tilde{p}_i\tilde{r}_i)} \right|^2 d^4\tilde{r}_i = \mathcal{F}[R(0)]$$

and:

$$P(\tilde{p}_1) \cdot P(\tilde{p}_2) = |\mathcal{F}[R(0)]|^2$$

so that the correlation function becomes finally:

$$\begin{aligned} C_{12}(\tilde{q}) &= +\frac{|\mathcal{F}[R(\tilde{q})]|^2}{|\mathcal{F}[R(0)]|^2} \quad \text{for bosons} \\ &= -\frac{|\mathcal{F}[R(\tilde{q})]|^2}{|\mathcal{F}[R(0)]|^2} \quad \text{for fermions} \end{aligned}$$

It is usually more convenient to represent the correlation function $R_{12}(\tilde{q})$ defined as:

$$R_{12}(\tilde{q}) = 1 + C_{12}(\tilde{q}) \tag{10}$$

From the preceding relations we conclude that the relative four-momentum dependence of the correlation function for identical particles is determined by the spatial dependence of the emitting region. It is necessary however to make an assumption about the general shape of the source density distribution. A stationary gaussian distribution is one of the most commonly used parametrisations:

$$\rho(\vec{r}, t) = \frac{1}{\pi^2 R^3 \tau} e^{\left(-\frac{\vec{r}^2}{R^2} - \frac{t^2}{\tau^2}\right)} \tag{11}$$

where R and τ are the radius and the lifetime of the source. The Fourier transform of 11 is:

$$\mathcal{F}[\rho(\vec{r},t)] = e^{\left(-\frac{q^2R^2}{4} - \frac{E^2\tau^2}{4}\right)}$$

so that the correlation function defined by equation 10 can be written as:

$$R_{12}^{\text{Gauss}}(\vec{q},E) = 1 \pm e^{\left(-\frac{q^2R^2}{2} - \frac{E^2\tau^2}{2}\right)} \tag{12}$$

where $\vec{q} = |\vec{p_1} - \vec{p_2}|$ is the relative momentum and $E = |E_1 - E_2|$ the relative energy of the particles. For bosons the correlation function isa maximum at zero relative momentum (equal to 2 at $\vec{q} = 0$) and decreases with increasing $\vec{q}$, the rate of decrease being related to the space and time characteristics of the source. For fermions the correlation function is a minimum at $\vec{q} = 0$.

Another very often-used parametrization of the source density distribution has been proposed by Kopylov and Podgoretski [10]. In their model, the particles are emitted from a spherical surface at rest with radius R, which contains a uniform distribution of independent massive point-like oscillators decaying exponentially with mean lifetime τ. They deduced the following form for the correlation function:

$$R_{12}^{\text{KP}} = 1 \pm \left[\frac{2J_1(Rq_t)}{Rq_t}\right]^2 \cdot \frac{1}{1+(\tau E)^2} \tag{13}$$

where q_t is the transverse part of $\vec{q}$ with respect to the direction of motion of the two-particle system, and $J_1(Rq_t)$ is a Bessel function of first order. It can be shown that there exists a simple relation between the parameters R in formulae 12 and 13:

$$R_{\text{KP}} = 2R_{\text{Gauss}}$$

Another representation of the source distribution is a special case of 12 where the source lifetime is taken equal to zero, and the relative momentum is split into its transverse (q_T) and longitudinal (q_L) components with respect to the beam axis:

$$R_{12}^{\tau=0}(q_T,q_L) = 1 \pm e^{\left(-R_T^2q_T^2 - R_L^2q_L^2\right)^2} \tag{14}$$

Figure 9 shows several correlation functions measured for identical charged pions in π^+p reactions at 16 GeV/c [11] and fitted to the Kopylov-Podgaretski formula (equation 13). An important feature to notice is that the correlation function never reaches the expected value of 2 at zero relative momentum. Therefore a new parameter λ has been introduced in the correlation function:

$$R_{12}(\tilde{q},\lambda) = 1 + \lambda C_{12}(\tilde{q}) \tag{15}$$

Although, the interpretation of λ is not unique, it could reflect the degree of coherence or its inverce, the degree of chaoticity of the source.

So far, we have only considered the case where the particles are emitted independently of each other. In the case of a coherent emission we have to rewrite $P(\tilde{p_1},\tilde{p_2})$ in relation 7 as a coherent sum of the two particle amplitudes:

$$P(\tilde{p_1},\tilde{p_2}) = \frac{1}{2}\left|\int_{\text{source}} \Psi_{12}(\tilde{p_1},\tilde{p_2})\,\rho(\tilde{r_1})\,\rho(\tilde{r_2})\,d^4\tilde{r_1}d^4\tilde{r_2}\right|^2$$

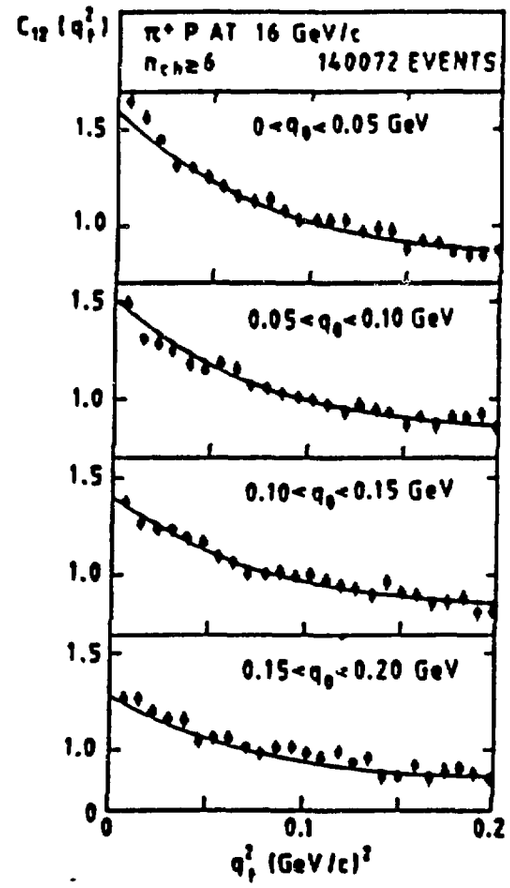

Figure 9: *The correlation function for pairs of particles of same charge versus q_T^2, for different regions of the energy difference q_0, between the particles. The lines show the result of a fit to formula 13. From ref. [12].*

Replacing $\Psi_{12}(\vec{p}_1, \vec{p}_2)$ by its expression in 10 we end up with:

$$\begin{aligned} P(\vec{p}_1, \vec{p}_2) &= |\mathcal{F}[\rho(\vec{p}_1)] \cdot \mathcal{F}[\rho(\vec{p}_2)]|^2 \quad \text{for bosons} \\ &= 0 \quad \text{for fermions} \end{aligned}$$

and the correlation coefficient becomes:

$$\begin{aligned} C_{12}(\vec{q}) &= 1 \quad \text{for bosons} \\ &= 0 \quad \text{for fermions} \end{aligned}$$

Thus for a coherent emission the correlation function is uniform. In the case of a mixing between chaotic and coherent emission, the coherence will tend to reduce the correlation function. In such an interpretation λ would then reflect the degree of coherence of the source:

$$\lambda = \frac{N_C}{N_I + N_C} = C_{12}(0)$$

where N_C and N_I are the number of pairs produced coherently and incoherently respectively.

But as I mentioned earlier, many other things may affect the λ parameter. Anyway it is rather tricky to measure the correlation function at zero relative momentum and the extraction of λ from the data may be model-dependent. On the other hand, final state interactions which we have neglected so far, or resonance decay may mask the coherent production, especially the Coulomb interaction between two like particles.

In high-energy physics, where there is enough energy available to excite nucleonic resonances or to create unstable particles, the contribution to the correlation function from their decay becomes important. This contribution will smear out the correlation and can be included in the parameter λ.

Final state interactions have to be considered wherever one studies correlations of particles subject to Coulomb and strong interaction, since they are travelling at close distance to each other. The Coulomb corrected correlation coefficient can be obtained easily as follows :

$$C_{12}^{\text{Coulomb}}(\vec{p}_1, \vec{p}_2) = G(\vec{p}_1, \vec{p}_2) \cdot C_{12}(\vec{p}_1, \vec{p}_2)$$

where G is the Gamow factor defined as :

$$G(\vec{p}_1, \vec{p}_2) = \frac{2\pi\eta}{e^{2\pi\eta} - 1}$$

η is the Sommerfeld factor:

$$\eta = \frac{\alpha m}{|\vec{p}_1 - \vec{p}_2|} \quad ; \quad \alpha = \frac{e^2}{\hbar c}$$

and m is the mass of the particle. The Coulomb interactions between the emitted particles and their source have not yet been considered systematically. It is believed that for pions the strong interaction is weak enough to be generally neglected. But for hadrons like protons, strong interactions will completely change the aspect of the correlation function. As we shall see, source parameters can still be extracted but the effect is not strictly an HBT effect any more.

Before coming to this peculiar aspect of particle correlations, I will quickly review the experimental status of source sizes deduced mainly from $\pi - \pi$ correlations measured over a broad range of bombarding energies.

2.2 HBT effect in identical particle correlations : experiment

Experimentally the correlation function is constructed from the singles yield $Y_i(\tilde{p}_i)$ of particles with four momentum $\tilde{p}_i$ and from the coincidence yield $Y_{12}(\tilde{p}_1, \tilde{p}_2)$ as follows:

$$R_{12}^{exp}(\tilde{q}) = N \frac{\sum Y_{12}(\tilde{p}_1, \tilde{p}_2)}{\sum Y_1(\tilde{p}_1) \cdot \sum Y_1(\tilde{p}_2)}$$

The sum in the numerator of the above relation is taken over all pairs of particles with four-momentum $\tilde{p}_1$ and $\tilde{p}_2$ with a given value $\tilde{q}$ for their relative four-momentum. The normalization factor N is chosen so that $R_{12}^{exp}(\tilde{q}) = 1$ at large relative four-momentum. The difficulty in evaluating the denominator lies in finding an "uncorrelated" reference. This can be done by using the random coincidences, or by selecting pairs of particles from different events. We can also see that the way the normalization factor is determined can influence the value of the coherence parameter or even modify the width of the measured correlation function. The analysis of the measured correlation function is then made according to formula 15 with one of the source parametrisations 12, 13, or 14. Because of limited statistics most authors assume sources with zero lifetime. Therefore possible lifetime effects are hidden and mocked-up by an effective spatial extension of the source.

2.2.1 High energy elementary particle collisions

In this type of collisions the source of particles is some kind of hadronic fireball which expands with time. The source characteristics which can be determined by particle (mainly charged pion) correlation studies correspond to the freeze-out density when the particles leave the source after (the final ultimate collision). This kind of approach to hadron dynamics provides a very important tool to clarify the reaction mechanism of multiparticle events and could help to disentangle their string structure (see for example reference [12]).

A systematic analysis of the available data (see the compilation in references [12] and [13]) shows that the correlation function does not remember the initial colliding system for systems as different as $p\bar{p}, pp, \bar{p}\pi, Kp$ and $e^+e^-, \mu p$ and νp. The deduced spatial extension of the source is always found to be around 1 fm and to not depend strongly upon the bombarding energy. Some authors could extract a lifetime of the order of 1-2 fm/c. In any case λ is found to be almost constant and smaller than unity but this effect can be attributed only tentatively to some coherence in the source.

2.2.2 Relativistic nucleus-nucleus collisions

In this field of nuclear physics, the source of pions which gives rise to correlation effects is the participant zone, where the nucleons of the projectile and target overlap. One thus expects a dependence of the source spatial extension on the size of the projectile. Such a dependence has indeed been observed as can be seen in fig. 10 which shows the measured radius of the source in a variety of collisions with projectiles ranging from proton to Krypton at energies of several GeV per nucleon.

It is interesting to note that the measured source radius is slightly larger than the size of the projectile ; this may indicate that the participant-region thermal freeze-out density is larger than the normal nuclear density. The same conclusion could be drawn from plastic ball data [14]. In Ca + Ca and Nb + Nb collisions at 400 MeV/u, the variation of the source size as a function of the proton multiplicity N_p (fig. 11) has been extracted from p-p

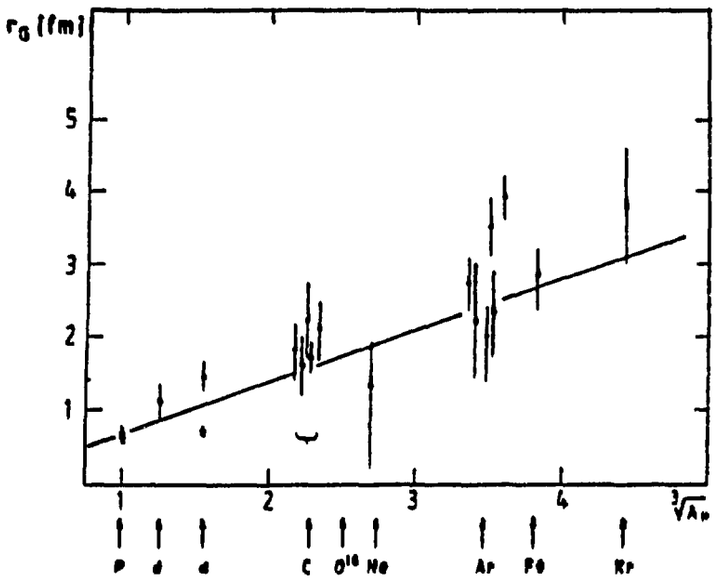

Figure 10: *The radius parameter (Gaussian fit) as a function of the cubic root of the number of nucleons in the projectile. The solid line indicates the radius of the projectile,* $R_p = 0.7A_p^{\frac{1}{3}}$ *fm. From ref. [12].*

correlations and parametrized as follows :

$$R = \frac{r_0 \left(N_p \frac{A}{Z}\right)^{\frac{1}{3}}}{\sqrt{\frac{5}{2}}} \tag{16}$$

where r_0 is the reduced root-mean-square radius. The fit to the data gives a value of 1.9 fm for $r_0$which compares to 1.2 fm for normal nuclei. The deduced increase in density is of the order of 25%. It is also found that the source size decreases with increasing energy of the particle pair ; this could be interpreted by saying that faster particles are emitted at an earlier stage of the expansion phase of the participant zone. But since the time is not explicitly included in the fit to the data it could also be due to a time dependent expanding source.

2.3 Ultrarelativistic nucleus-nucleus collisions

Pion interferometry has been suggested as an interesting tool to study the formation of a quark-gluon plasma [15]. In ultrarelativistic collisions the hot matter is produced in a cylinder along the beam axis. Two directions are then considered for the pion source, the outward direction, perpendicular to the cylinder and parallel to the pion direction and the sideward direction perpendicular to both the cylinder and the pion direction (see fig. 12). In the case of a hot pion gas, because of the multiple scattering of pions, one expects the pion source to have an almost equal size in the sideward and outward directions. Were a plasma to be formed, its conversion to the hadronic phase being slow, the pions will

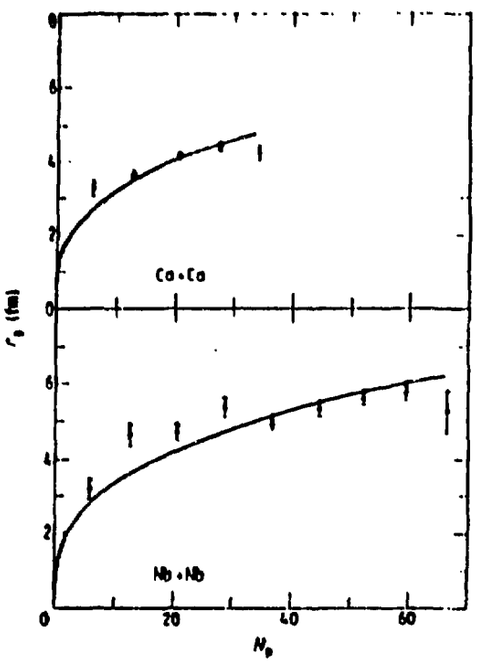

Figure 11: *Source radii as a function of proton multiplicity for two systems at 400 MeV/u. The curves are fits using equation 16.*

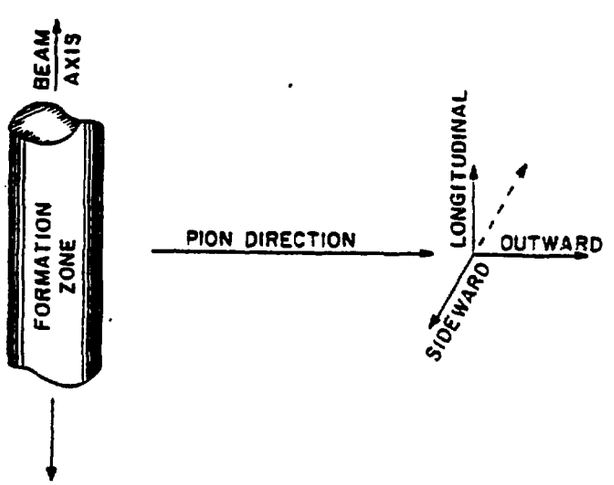

Figure 12: *Coordinate system for pions emerging from ultrarelativistiv heavy ion collision. From ref. [15].*

be emitted at a reduced rate and will not rescatter much. Therefore one expects a small sideward dimension and a larger outward dimension.

The NA35 experiment has provided an estimate of the pion source size in this energy domain [16]. It studied the reaction ^{16}O+Au at 200 GeV/nucleon. The correlation function was constructed for various bins in rapidity and interpreted according to equations 15 and 13 or equations 15 and 14. A comparable dimension of the source in the longitudinal and transverse direction is found . Most importantly, in the centre-of-mass rapidity region, the radius, the lifetime and the chaoticity parameter are found to increase strongly: $R_T \approx R_L \approx 8$ fm, $\lambda \approx 0.8$, $\tau \approx 6$ fm/c. This may be an indication that a thermalized fireball was formed and has expanded toward a low energy density at which the pions decouple.

The next energy domain to consider is the intermediate-energy one. There, the pion multiplicity is much too low to undertake pion correlation measurements. But the hadron multiplicity is large and a lot of work has been published on proton-proton correlations as well as on more complex particles and even non-identical particles. There the correlation function is dominated by final state interaction and the source size is not so much deduced from the HBT effect but rather from the intensity of resonances, if they exist, in the two particles system. How this is done is shown in the next section.

2.4 Final state interaction and resonances

In the presence of final state interactions due to the Coulomb and nuclear force, one needs to rewrite $\Psi_{12}(\vec{p_1}, \vec{p_2})$ in equation 7 in order to satisfy the Schrödinger equation for the two-particle system including a Coulomb and nuclear potential. In the case of a system of two protons :

$$\Psi_{12}(\vec{p_1}, \vec{p_2}) = \frac{1}{4}\left|{}^1\Psi_q(\vec{r})\right|^2 + \frac{3}{4}\left|{}^3\Psi_q(\vec{r})\right|^2 \tag{17}$$

where Ψ_{12} describes the relative motion in the outgoing channel with the singlet and triplet spin components. The statistical weight corresponds to a statistical distribution of the proton spins. The interaction of the particles with the surrounding nuclear medium is neglected.

A widely used source density distribution has been proposed by Koonin [17]:

$$\rho(\vec{r}, t) = \frac{1}{\pi^{\frac{3}{2}} r_0^3} e^{\left(-\frac{\vec{r}-\vec{V_0}t}{r_0^2}\right)} \cdot \frac{1}{\pi^{\frac{1}{2}} e^{\left(-\frac{t^2}{\tau^2}\right)}}$$

r_0, τ are the source spatial and temporal extensions and $\vec{V_0}$ is the laboratory velocity of the particles. We further assume that the two particles are emitted with almost equal momenta, so that the correlation coefficient defined in relation 6 can be written as:

$$C_{12}(\vec{q}) = \frac{1}{(2\pi)^{\frac{3}{2}} r_0^2 \rho} \int_{\text{source}} d\vec{r}\, e^{\left\{r^2 - \left(\frac{\vec{r}\cdot\vec{V'}\tau}{\rho}\right)^2\right\}/2r_0^2} \left|\Psi_{12}(\vec{q})\right|^2 \tag{18}$$

where $\Psi_{12}(\vec{q})$ is given by relation 17 in the case of the proton-proton system. $\vec{V'}$ is the velocity of the two particle system seen in the frame of the emitter and:

$$\rho = \left\{r_o^2 + \left(\vec{V'}\tau\right)^2\right\}$$

Thus, in the laboratory system the source will look prolate in the direction of the moving particles with an elongation equal to ρ. One then ends up with a new parameter, namely the velocity of the source, when its lifetime is not zero. Koonin has calculated the correlation function from relation 18 for various values of the source parameters. The results are shown on fig. 13. At low relative momentum ($q < 100$ MeV/c) the dip is due to a combination of three effects:

- the Coulomb repulsion which prevents the two protons from having parallel trajectories;
- the Pauli exclusion principle which prevents two protons from occupying the same quantal state;
- the HBT effect due to the Fermi-Dirac statistics.

Around $q \sim 20$ MeV/c, the correlation becomes attractive because of the strong-force attraction between the two protons in the singlet state $^1S_0$. At large relative momentum, above $q \simeq 80$ MeV/c, the two protons are too far apart to feel any other interaction than the Coulomb one. Although the quantum statistical effect is a part of the interaction between the two particles it is possible to extract information about the source extension form the correlation function as shown in fig. [?]. The magnitude of the correlation in the resonance region increases with decreasing r_0, the spatial extension of the source.

This property has been widely used to determine the source size of the protons emitted in heavy ion collisions at intermediate energies. As a general trend, it is observed that for fast protons, the source size is always comparable with the target one which might identify the source with the participant zone. For slow protons, the size of the source becomes larger than the size of the projectile(see fig. 14). This effect can be attributed, as we shall see later on, to possible finite lifetime effects . This kind of correlations which relies upon final state interactions, can be extended to complex particles, and even the correlation for non- identical particles can provide useful information. In that case, the HBT effect is no longer present and information about the source is obtained through the magnitude of the resonance reflecting the strength of the two-particle interaction. However, because of their larger reaction cross sections, complex particles may be expected to interact for a larger reaction time and may therefore be emitted from a source of lower density than the proton one. It becomes attractive therefore to study correlations between different particles emitted in the same reaction, to get a hold on the dynamical expansion of the reaction zone.

Figure 15 shows an example of the correlation function measured for the systems $\alpha - \alpha$ and $p - \alpha$. The observed peaks correspond to particle unstable excited states in compound systems.

2.5 HBT effect and the timescale of particle emission

I have already mentioned in the preceding section that the apparent source size extracted from the correlation function measured for low energy protons is larger than the size of the projectile and than the size obtained with fast protons. Because of the experimental difficulty in disentangling the spatial and temporal contributions to the correlation function this effect could be attributed to a source dilation as well as to its finite lifetime. Slow protons are most likely emitted from a thermalized source, therefore the second interpretation may be the correct one. Because of the thermal character of the source it is expected that

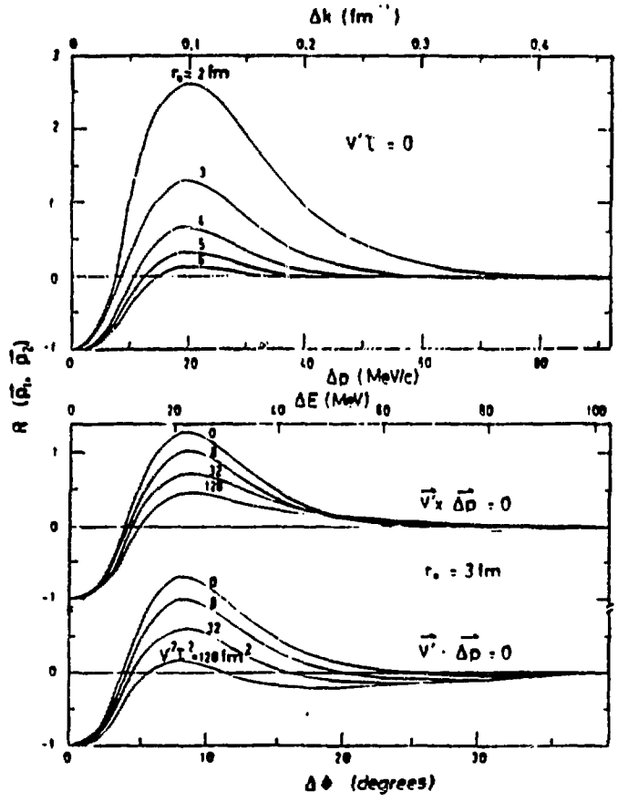

Figure 13: *Upper portion: the two-proton correlation function for various values of* r_0 *when* $V'\tau = 0$. *Lower portion: the correlation function for various values of* $V'\tau$ *when* $r_0 = 3$ *fm. From ref [17].*

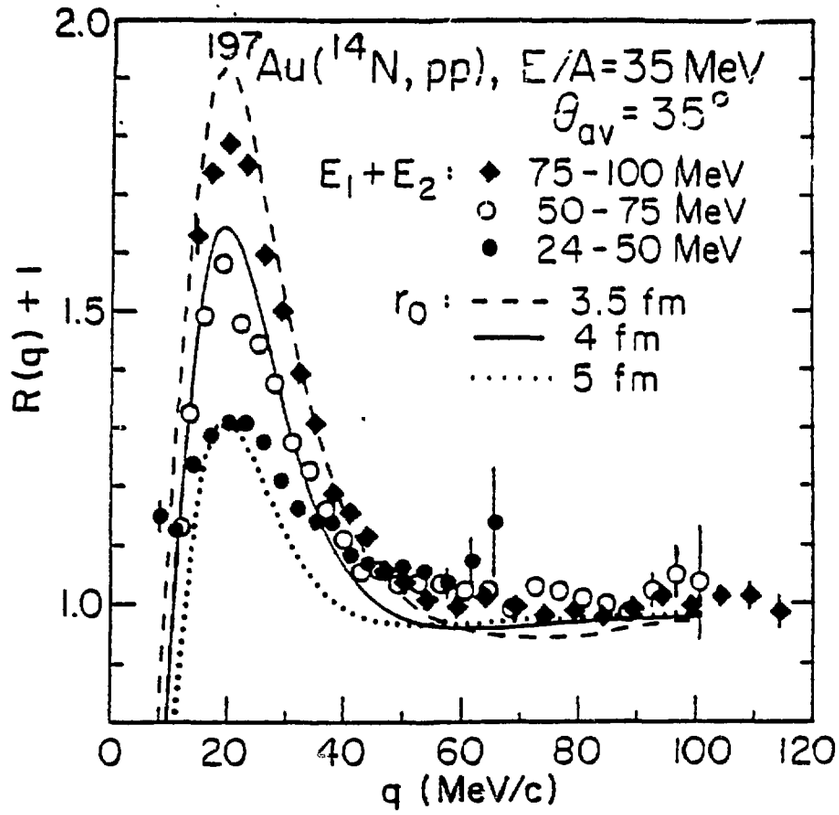

Figure 14: *Correlation function for the system p-p measured in the reaction N+Au at 35 MeV/nucleon and for different values for the energy of the protons. The fit are made with equation 18. From ref. [13].*

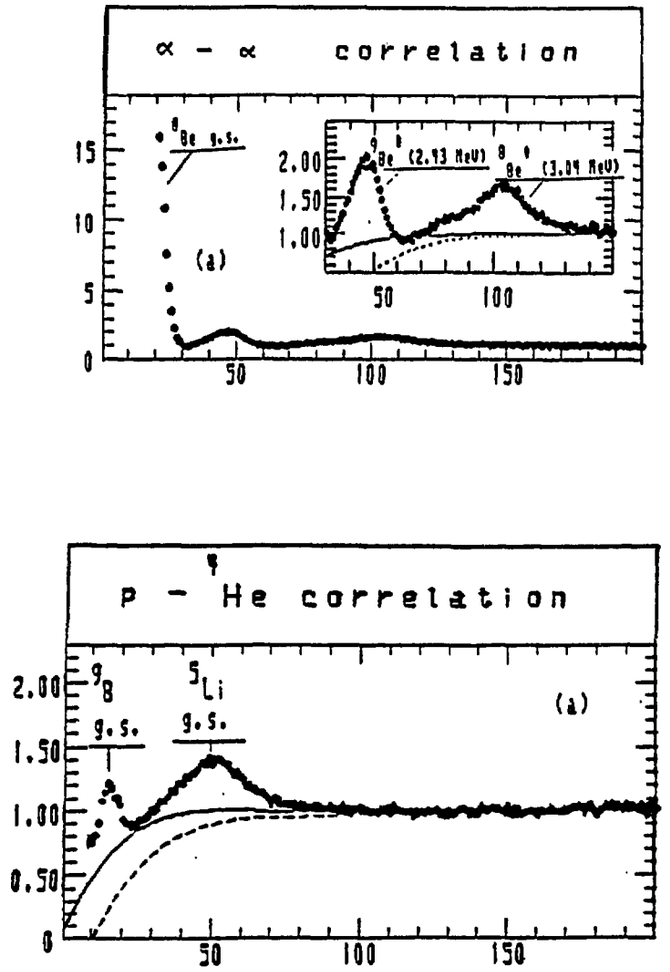

Figure 15: *Correlation function for the system $\alpha-\alpha$ (upper) and $p-\alpha$ (lower). The origin of the resonances is indicated on the figure. From ref. [18].*

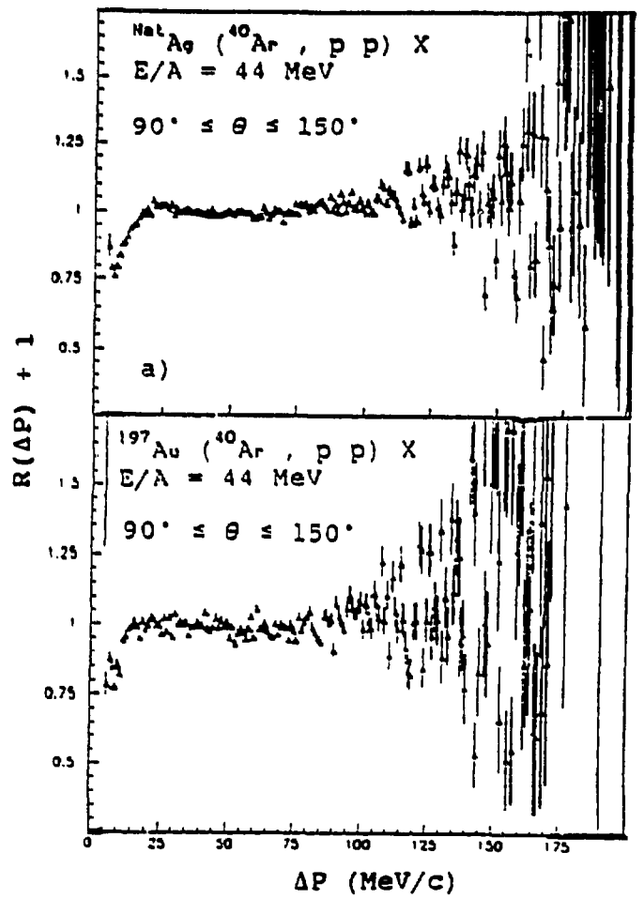

Figure 16: *Correlation function measured for the p-p system in Ag+Ar (upper) and Au+Ar (lower) at 44 MeV/nucleon at backward angles. From ref. [19].*

the sequential emission will reduce the final state nuclear interaction and that, at the same time, because of the high chaoticity of the source, the pure quantum effect (HBT effect) will be enhanced.

It has therefore been proposed to use the properties of particle correlations to measure the lifetime of the thermalized source which coincides with the compound nucleus at the lower bombarding energies. Experimentally one selects thermal emission by selecting slow particles, or by measuring the particles at backward angles [19] or by selecting reactions where a compound nucleus is formed [20]. Figure 16 shows the p-p correlations measured at backward angles in the reaction Ar+Au at 44 MeV/nucleon. When compared to the correlation function shown in fig. 14 one observes the complete disappearance of the enhancement in the resonance region at $q \simeq 20$ MeV/c.
This tells us that the particles are no longer subject to the nuclear interaction and gives us accordingly a clock for the reaction. The correlation function tends towards 0.5 at zero relative momentum which is expected from pure quantum statistics and spin weighting. Moreover since the Coulomb repulsion is also a part of the interaction, it will contribute to the anticorrelation and it becomes difficult to distinguish the two contributions. From these observations one can conclude that the two protons may be emitted sequentially with an

average delay time large enough to totally damp the short range nuclear interaction. A fit to the data using relation 13 gives $R \simeq 7$ fm and $\tau \simeq 12 \cdot 10^{-22}$ s. Similar results have been obtained at much lower bombarding energies ($E \leq 10$ Mev/nucleon) [20], where heavy-ion reactions proceed mainly via fusion to give a compound nucleus at finite temperature. The deduced evaporation lifetime is of the order of $1.5 \cdot 10^{-21}$ s.

I should also mention the pioneering work which has been performed some ten years ago at the MPI of Heidelberg [21]. To my knowledge, it was the very first attempt to apply intensity interferometry in low energy nuclear physics. They used $p-p$, $\alpha-\alpha$ and $p-\alpha$ correlations at small relative momenta to deduce the lifetime of highly excited compound nuclei formed in fusion reactions, or of excited fragments formed in deep-inelastic collisions. It was also the first attempt to measure nuclear lifetimes below 10^{-20} s. They succeeded in measuring lifetimes of the order of $3 \cdot 10^{-22}$ s.

3 Conclusion

It has been shown in this lecture how a very general and new principle can be applied to measure large stellar objects as well as tiny objects at the scale of the nucleus. Nevertheless, it is clear that the application of the HBT effect in nuclear physics has a handicap to overcome due to the probe. The particles for which the correlations are studied are subject to nuclear and Coulomb interactions which often render the interpretation of the effect uncertain. Therefore we have considered the possibility of using photons as a probe since they are the only undistorted probe of nuclear reactions and since their origin is rather well localized in space and time (see V. Metag in this conference). In the next lecture, R. Ostendorf will demonstrate the feasibility of such experiments.

References

[1] P.A.M. Dirac, The Principles of Quantum Mechanics, published by Oxford University, London.

[2] G.I. Taylor, Proc. Cambridge Philos. Soc., 15, (1909), 114; cited in H. Paul, Rev. Mod. Phys., 58, (1986), 209.

[3] R. Hanbury-Brown and R.Q. Twiss, Phil. Mag., 45, (1954), 663.

[4] R. Hanbury-Brown and R.Q. Twiss, Nature, 177, (1956), 27.

[5] R. Hanbury-Brown and R.Q. Twiss, Nature, 177, (1956), 1046.

[6] R. Hanbury-Brown FRS, The Intensity Interferometer, edited by Taylor & Francis Ltd, London, (1974).

[7] H. Paul, Rev. Mod. Phys., 58, (1986), 209.

[8] G. Goldhaber, W.B. Fowler, T.F. Moang, T.E. Kalogeropoulos and W.M. Powell, Phys. Rev. Lett., 3, (1959), 181.

[9] G. Goldhaber, S. Goldhaber, W. Lee and A. Pais, Phys. Rev., 120, (1960), 300.

[10] G. Kopylov and M. Podgoretski, Sov. J. Nucle. Phys., 18, (1974), 336.

[11] M. Deutschmann et al., Nucl. Phys., B204, (1982),33.

[12] B. Lörstad, Int. J. Mod. Phys., A4, (1989), 2861.

[13] D.H. Boal, C.K. Gelbke and B.K. Jennings, preprint MSUCL-726, Michigan State University, May 90, to be published in Rev. Mod. Phys.

[14] H. Gutbrod, A.M. Poskanzer and H.G. Ritter, Rep. Prog. Phys., 52, (1989), 1267.

[15] G.F. Bertsch, Nucl. Phys., A498, (1989), 173c.

[16] T.J. Humanic and NA35 Collaboration, Z. Phys., C38, (1988), 79.

[17] E. Koonin, Phys. Lett., 70B, (1977), 43.

[18] A. Kyanowski, Thèse, T87-03, GANIL.

[19] D. Ardouin, Rapport Interne, LPN 89-02, Nantes

[20] P.A. De Young, M.S. Gordon, Xiu qin LU, R.L. McGrath, J.M. Alexander, D.M. de Castro Rizzo, and L.C. Vaz, Phys. Rev., C39, (1989), 128.

[21] W. Kühn, Lecture Notes in Physics, Vol. 117, Springer Verlag 1979.